A Longwave Broadband QME Based on ARM Pyrgeometer and AERI Measurements

S. A. Clough, A. D. Brown, C. Andronache, and E. J. Mlawer
Atmospheric and Environmental Research, Inc.
Cambridge, Massachusetts

T. R. Shippert and D. D. Turner
Pacific Northwest National Laboratory
Richland, Washington

D. C. Tobin, H. E. Revercomb, and R. O. Knuteson
University of Maryland
College Park, Maryland

Introduction

Accurate modeling of the downwelling longwave flux at the surface is critical to our understanding of a number of important issues: the earth's energy balance; processes at the atmosphere's lower boundary including ice melt and ocean forcing; and evaluating our ability to model atmospheric fluxes for dynamical models including numerical weather prediction and climate models. Under the Atmospheric Radiation Measurement (ARM) Program, there has been a concerted effort (Brown et al. 1998) to evaluate the modeling of the downwelling zenith spectral radiances using Atmospheric Emitted Radiance Interferometer (AERI) measurements (Revercomb et al. 1997) and the line-by-line radiative transfer model (LBLRTM) (Clough and Iacono 1995). Up to this point, there has not been a comparable effort to extend this type of analysis to the downwelling fluxes at the surface, which are of interest to the broader community.

For the Quality Measurement Experiment (QME) described here, the three major components are the radiometric measurements, the radiative transfer modeling, and the specification of atmospheric state. The first objective of this QME is to evaluate the performance of the three components as implemented at the Southern Great Plains (SGP) ARM site. A second objective is to develop a database of spectral downwelling fluxes that can be used by the community to evaluate radiative transfer models beyond those being used here. In the present QME, a spectral component is being retained to provide information on the spectral regimes and their associated physical processes that give rise to the differences between measured and modeled flux.

Description of Components

Measurements: Two instruments are being used to obtain the downwelling flux measurements: the pyrgeometer, which measures the flux for the full hemispherical solid angle and the entire longwave spectrum, and the AERI interferometer, which measures the zenith spectral radiance from 550 cm^{-1} to

3000 cm^{-1}. For the present application, the AERI measurements must be extended spectrally to cover the entire longwave regime, and the downwelling spectral flux must be obtained from the zenith radiance observation. The method for achieving this objective is discussed at length below.

Radiative Transfer Models: Two radiative transfer models are being used in this QME: rapid radiative transfer model (RRTM) (Mlawer et al. 1997) and the LBLRTM. RRTM covers the entire longwave spectrum from 10 cm^{-1} to 3000 cm^{-1} in 16 bands. The model is capable of calculating both fluxes and radiances assuming a plane parallel homogeneous atmosphere.

Specification of Atmospheric State: The temperature profile for the model calculations is obtained directly from the radiosonde observation. As is the case for the AERI/LBLRTM QME, the water vapor profile is obtained by scaling the specific humidity obtained from the radiosonde to attain agreement with the water vapor column obtained from the microwave radiometer (MWR) (Clough et al. 1999). The temporal sampling grid for the present comparison between modeled and measured fluxes is set by radiosonde release times.

Procedure

The calculations done for this experiment are done in concert with the ones performed for the longstanding AERI/LBLRTM QME. Since the AERI is located in a trailer at the SGP Cloud and Radiation Testbed (CART) site, the radiation path of the AERI is unique in that it includes a short horizontal piece from an outdoor reflecting mirror to the indoor interferometer. Therefore, for the AERI/LBLRTM QME, the LBLRTM calculations of monochromatic downwelling surface radiance (zenith) from 500 cm^{-1} to 3000 cm^{-1} are performed in two parts: First, using the atmospheric profile as defined above, the atmospheric transmittance T_{lblrtm_atm} and surface radiance R_{lblrtm_atm} are computed; and, second, the transmittance $T_{lblrtm\_AERI\text{-}path}$ and radiance $R_{lblrtm\_AERI\text{-}path}$ corresponding to the horizontal AERI radiation path are calculated. Then, the final monochromatic radiance is computed by $R_{lblrtm\_AERI} = R_{lblrtm\_AERI\text{-}path} + T_{lblrtm\_AERI\text{-}path} R_{lblrtm\_atm}$. R_{lblrtm_AERI} will differ appreciably from R_{lblrtm_atm} only for relatively opaque spectral elements. Finally, the calculated radiance that is compared to the AERI observation is obtained by applying the appropriate instrument functions to the monochromatic calculations.

Using the same atmospheric profile as for the LBLRTM calculation, the rapid radiation model RRTM is also run to obtain both downwelling radiances and fluxes for the 16 bands in the model. For each band, the zenith radiance R_{rrtm_atm} and the flux F_{rrtm_atm} (sum in quadrature of radiances computed at three angles) are calculated.

For the current experiment, it is the flux corresponding to the atmospheric radiance R_{lblrtm_atm} that is of interest. Both the LBLRTM-computed and AERI radiances must be converted to fluxes, but first two issues with the AERI radiances must be resolved first:

1. Effective AERI atmospheric radiances are obtained by removing effects of the horizontal piece of the AERI radiation path using

$$R_{AERI\_atm} = (R_{AERI\_measured} - R_{lblrtm\_AERI\text{-}path}) / T_{lblrtm\_AERI\text{-}path}.$$

For opaque spectral regions this equation is not solvable, corresponding to the absorption along the horizontal AERI path of all radiation originating in the atmosphere. Therefore, R_{AERI_atm} is replaced by R_{lblrtm_atm} for opaque spectral elements.

2. The AERI spectral radiances are extended to 500 cm^{-1} (from 550 cm^{-1}) using LBLRTM calculated radiances R_{lblrtm_atm}

The flux-to-radiance ratio for downwelling radiation depends on the transmittance of the atmosphere associated with the given spectral element. For opaque conditions, the radiation field is isotropic and the flux F is equal to p R. For non-opaque conditions, the zenith downwelling radiance is a minimum of the radiation field and must be multiplied by a factor greater than p to obtain the flux. For the assumption that each downwelling spectral radiance is from a single radiating layer, the flux-to-radiance ratios g (defined by F = g p R) can be straightforwardly computed as a function of layer transmittance. These factors are shown in Figure 1. Therefore, the first step used in the conversion to flux of each R_{lblrtm_atm} and R_{AERI_atm} is the application of the factor g corresponding to the transmittance T_{lblrtm_atm}. When summed over each spectral band of RRTM, the ratio of the flux (obtained by this method) and radiance is not necessarily equal to the desired ratio F_{rrtm_atm} / R_{rrtm_atm} for that band. Therefore, a small correction of equal magnitude within each RRTM band is made to each spectral flux so that the summed flux-to-radiance ratio is equal to the one computed by RRTM for that band.

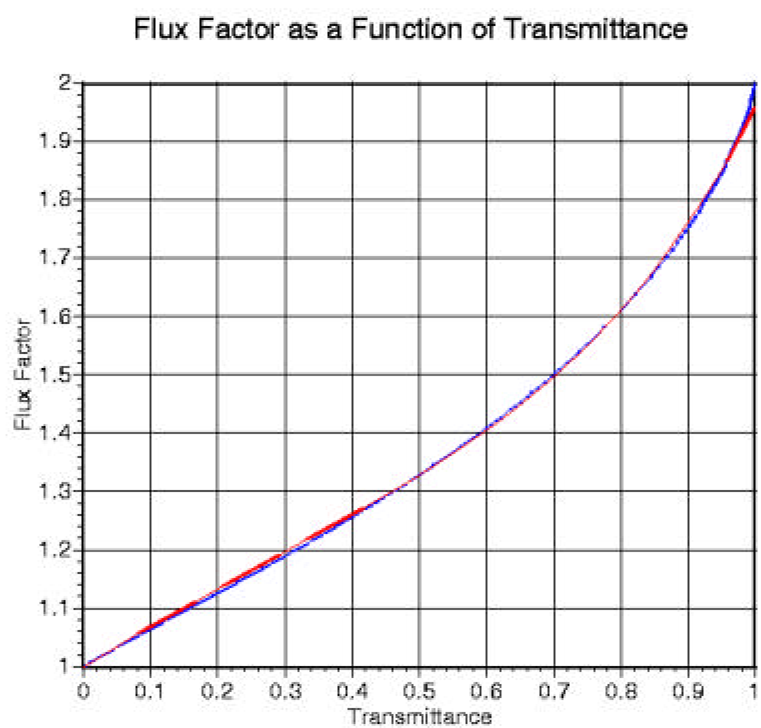

Figure 1. For downwelling radiation from a single-Radiating layer, the ratio of flux to radiance (* pi) as a function of transmittance.

The factors in Figure 1 are most appropriately applied to convert radiance to flux if the atmosphere can be treated as a single radiating layer. This is not the case for the radiances in the 980 cm^{-1} to 1080 cm^{-1} band of RRTM due to contributions to the downwelling surface radiation of water vapor in the troposphere and ozone in the stratosphere. For this reason, an extension of the method described above is used in this band to convert the AERI and LBLRTM spectral radiances to fluxes.

The resulting AERI and LBLRTM spectral fluxes are integrated and stored in 10 cm^{-1} bins, useful for intercomparison of radiative codes in climate models (ICRCCM) type intercomparisons (Ellingson and Fouquart 1991), and in the RRTM bands. To obtain broadband longwave fluxes, the fluxes computed by RRTM in the opaque region from 10 cm^{-1} to 500 cm^{-1} are used as AERI and LBLRTM flux values for that spectral range. Figure 2 shows the fluxes measured by the pyrgeometer, the AERI broadband fluxes, and the RRTM-computed broadband fluxes for a time period in 1997-1998. The seasonal cycle in downwelling longwave flux is easily discernible. In Figure 3, differences in broadband flux are shown for the pyrgeometer, RRTM, and AERI relative to LBLRTM as a function of precipitable water vapor. The fluxes for RRTM and LBLRTM agree within 1 W/m^2 and show a slight trend with water vapor. The AERI-LBLRTM flux residuals are typically positive and <4 W/m^2 and show a quadratic dependence on water vapor. The fluxes measured by the pyrgeometer are higher than those calculated by LBLRTM by 2-10 W/m^2, with a typical difference between the pyrgeometer and the AERI fluxes of ~3 W/m^2, indicating that this broadband instrument measures longwave flux with an accuracy consistent with its expected error.

As mentioned above, the LBLRTM-computed fluxes are, in almost all cases, less than the AERI and pyrgeometer fluxes. Although this may be caused by a number of different biases in the measurements, models, and atmospheric state specification, one plausible reason for this behavior is that the model calculations lack a source of emitted radiation such as aerosols. This possibility has been investigated

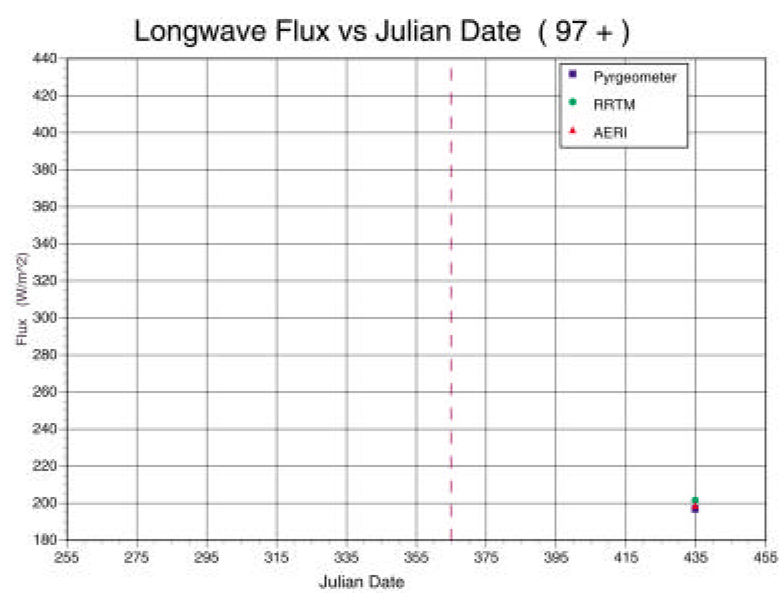

Figure 2. For September 1997 - March 1998, downwelling longwave fluxes from pyrgeometer, AERI, and RRTM calculations.

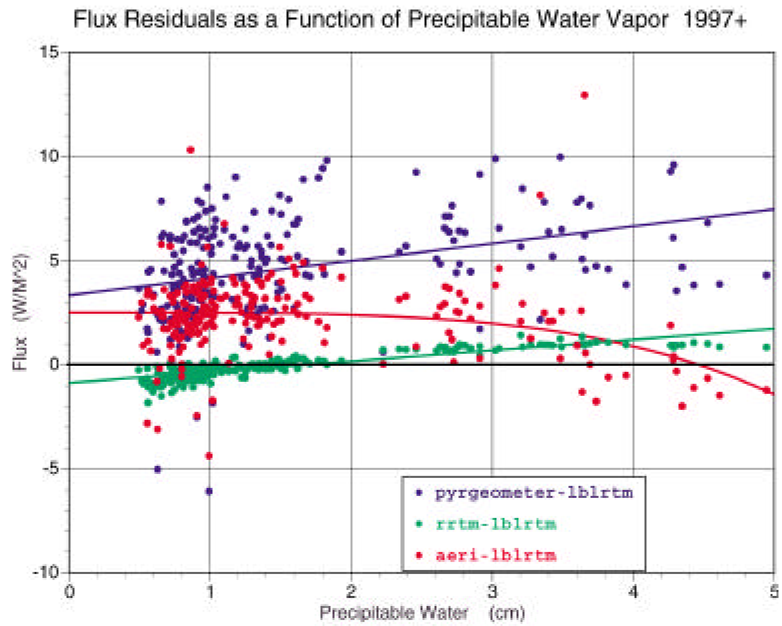

Figure 3. For September 1997 - March 1998, downwelling longwave flux differences (relative to LBLRTM calculations) for pyrgeometer, AERI, and RRTM calculations as a function of precipitable water vapor.

for a subset of the cases represented in Figure 2 by performing Moderate Resolution Transmittance (model) (MODTRAN) calculations (Berk at al. 1998) of longwave surface flux with and without aerosols. For each calculation, the longwave aerosol optical depth was determined from the visibility measured by the MFRSR and a rural aerosol was assumed. The result of these calculations suggests that the inclusion of aerosols in the model would increase longwave surface flux by less than 1 W/m^2 in most cases, not enough to explain all of the flux differences observed. The spectral regions in which the AERI-LBLRTM differences occur do correlate to some extent with the regions in which the increased flux due to aerosols occurs in the MODTRAN calculations, but that is inconclusive since the spectral pattern of other likely errors in the model (e.g., temperature, water vapor abundance, and spectroscopy) would also be similar.

The good agreement between the observation- and calculation-based determinations of broadband longwave flux leads to increased confidence in the measurements, model calculations, and the specification of the atmospheric state in the radiating column. In particular, the calculations by the rapid model RRTM can be considered accurate to the degree indicated in Figure 3, and the cooling rates computed by RRTM at all altitudes can be used by single-column modelers with a high level of confidence.

Future Enhancements

Using reasonable values for the upwelling surface flux, the calculations performed by RRTM also yield a top-of-the-atmosphere (TOA) flux product (by band and total) which would be useful for comparisons with Clouds and Earth's Radiant Energy System (CERES) (Charlock and Alberta 1996). The validity of this product will be strongly dependent on upper atmospheric water vapor and on upwelling surface flux in the 10-micron window. In addition, the methods used above should be able to be straightforwardly extended to apply to cloudy conditions and the shortwave region. Working with the Cloud Properties and the Cloud Parameterization and Modeling Working Groups, it is planned to extend these broadband comparisons to all aspects of radiation pertinent to ARM: clear and cloudy conditions; thermal and solar radiation; surface and top-of-the-atmosphere fluxes; and the SGP, North Slope of Alaska (NSA), and Tropical Western Pacific (TWP) CART sites.

References

Berk, A., L. S. Bernstein, G. P. Anderson, P. K. Acharya, D. C. Robertson, J. H. Chetwynd, and S. M. Adler-Golden, 1998: MODTRAN cloud and multiple scattering upgrades with applications to AVIRIS. *Remote Sens. Environ*., **65**, 367-375.

Brown, P. D., S. A. Clough, D. D. Turner, T. R. Shippert, R. O. Knuteson, H. E. Revercomb, and W. L. Smith, 1998: The status of the quality measurement experiments in the microwave, longwave, and shortwave. In *Proceedings of the Seventh Atmospheric Radiation Measurement (ARM) Science Team Meeting*, CONF-970365, pp. 499-504. U.S. Department of Energy. Available URL: http://www.arm.gov/docs/documents/technical/conf_9703/brown-97.pdf

Charlock, T. P., and T. L. Alberta, 1996: The CERES/ARM/GEWEX Experiment (CAGEX) for the retrieval of radiative fluxes with satellite data. *Bull. Amer. Meteor. Soc.*, **77**, 2673-2683.

Clough, S. A., P. D. Brown, D. D. Turner, T. R. Shippert, J. C. Liljegren, D. C. Tobin, H. E. Revercomb, and R. O. Knuteson, 1999: Effect on the calculated spectral surface radiances due to MWR scaling of sonde water vapor profiles, In *Proceedings of the Ninth Atmospheric Radiation Measurement (ARM) Science Team Meeting*, U.S. Department of Energy, Washington, D.C. Available URL: http://www.arm.gov/docs/documents/technical/conf_9903/clough-99.pdf

Clough, S. A., and M. J. Iacono, 1995: Line-by-line calculation of atmospheric fluxes and cooling rates, 2. Application to carbon dioxide, ozone, methane, nitrous oxide, and the halocarbons. *J. Geophys. Res.*, **100**, 16,519-16,535.

Ellingson, R. G., and Y. Fouquart, 1991: The intercomparison of radiation codes in climate models: An overview. *J. Geophys. Res*., **96,** 8925-8927.

Mlawer, E. J., S. J. Taubman, P. D. Brown, M. J. Iacono, and S. A. Clough, 1997: Radiative transfer for inhomogeneous atmospheres: RRTM, a validated correlated-k model for the longwave. *J. Geophys. Res*., **102,** 16663-16682.

Revercomb, H. E., F. A. Best, R. O. Knuteson, B. A. Whitney, T. P. Dirkx, R. G. Dedecker, R. K. Garcia, P. van Delst, W. L. Smith, and H. B. Howell, 1997: Atmospheric emitted radiance interferometer, Part I: Status, basic radiometric accuracy, and unexpected errors and solutions. In *Proceedings of the Sixth Atmospheric Radiation Measurement (ARM) Science Team Meeting*. U.S. Department of Energy, Washington, D.C. Available URL: http://www.arm.gov/docs/documents/technical/conf_9603/rev_96.pdf